PROCEEDINGS OF SCIENCE

Amplitude analysis of the $D^+ \to K^0_S \pi^+ \pi^0$ Dalitz plot

Peter Weidenkaff[*†]
Johannes Gutenberg University Mainz
E-mail: weidenka@kph.uni-mainz.de

We perform an analysis of the $D^+ \to K^0_S \pi^+ \pi^0$ Dalitz plot using a data set of 2.92 fb^{-1} of e^+e^- collisions at the $\Psi(3770)$ mass accumulated with the BESIII experiment, in which 166694 candidate events are selected with a background of 15.1%. The Dalitz plot is found to be well represented by a combination of six quasi- two-body decay channels [$K^0_S \rho^+$, $K^0_S \phi(1450)$, $\bar{K}^{*0}$, $\bar{K}_0(1430)^0$, $\bar{K}(1680^0 \pi^+$, $\bar{\kappa}^0 \pi^+$] plus a small nonresonant component. Using the fit fractions from this analysis, partial branching ratios are updated with higher precision than previous measurements.

XIIth International Conference on Heavy Quarks & Leptons 2014,
25-29 August 2014
Schloss Waldthausen, Mainz, Germany

[*]Speaker.
[†]For the BESIII collaboration

PoS(HQL2014)005

1. Introduction

The study of hadronic three-body charm decays provides a rich laboratory to investigate final-state interaction and interferences of intermediate-state resonances. A Dalitz plot analysis is the appropriate method here. It uses the minimum number of independent decay variables (usually two invariant masses squared) to visualize the dynamics in the decay. An amplitude analysis can then determine magnitudes and relative phases of the resonances, contributing to the decay.

The final state $K^0_S\pi^+\pi^0$ is a so called golden channel to study the $K^0_S\pi$ S-wave. Complementary analyses by CLEO-c and other experiments in the decay $D^+ \to K^-\pi^+\pi^+$ revealed a $\bar{\kappa}\pi$ contribution to th $K^-\pi^+$ S-wave. The final state $K^0_S\pi^+\pi^0$ was previously studied by MARKIII[1] with limited statistics, and no contribution from $\bar{\kappa}\pi$ was found. BESIII has collected a large data sample at the energy $\sqrt{s}$ =3.77 GeV and provides a clean environment to study D decays.

BESIII is a 4π detector with a geometrical acceptance of 93% and consists of the following components. The momentum and energy loss of charged tracks is measured in a small cell helium based multilayer drift chamber in a 1T magnetic field. The relative momentum resolution for a 1 GeV track is 0.5% and its energy loss is measured with a precision of 6%. The chamber has a radius of 81cm and is surrounded by two layers of plastic scintillator which is capable of measuring the flight time of particles with an accuracy of 80ps (in the barrel, end cap 110ps). This provides a $K\pi$ separation of 2σ for a 0.9 GeV track. Around the time-of-flight system, 6240 CsI(Tl) Crystals measure the energy of showers and neutral particles with a relative resolution of $2.5\%\sqrt{E}$ and their position with $0.6\text{cm}/\sqrt{E}$. Finally, surrounding the superconducting coil of the magnet are 9 layers of resistive plate chambers for muon identification. Further details can be found in [2]

2. Event selection

For this analysis we use our full data set of 2.92 fb^{-1} of e^+e^- collisions collected at 3.77 GeVwith the BESIII detector. At that energy neutral and charged D mesons are produced in the reaction $e^+e^- \to \Psi(3770) \to D\overline{D}$. The sample provides approximately 10^7 $D^0\overline{D^0}$ and 8×10^6 D^+D^- pairs.

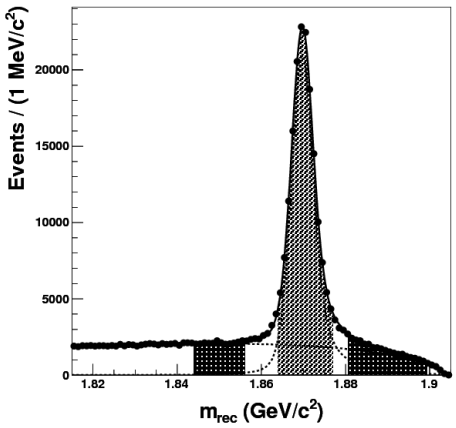

Figure 1: The recoil-mass distribution of $K^0_S\pi^+\pi^0$ candidates.

The K^0_S vertex is reconstructed through the decay $K^0_S \to \pi^+\pi^-$. It is required to be separated from the interaction point by 2σ. The pions are identified by their dE/dx measurement and their invariant mass needs to be in a 20 MeV window of the nominal K^0_S mass. The best candidate is then constrained to the nominal K^0_S mass.

Track candidates for the charged pion in the final state are required to come from the interaction point and are identified by combined information from TOF and dE/dx.

The π^0 candidate is reconstructed through its decay $\pi^0 \to \gamma\gamma$. Photons detected in the barrel region need to have a energy larger then 25 MeV and in the end cap at least 50 MeV. At least

one photon is required to be detected in the barrel region, and the invariant mass is required to be between 0.115 GeV and 0.15 GeV. Also the π^0 candidates are constrained to the nominal π^0 mass.

All three candidates are combined to a $D^{\pm}$ candidate with the requirement that the difference between the D^+ energy and the beam energy is between -73 MeV and 41 MeV. This energy difference is also used to select the best candidate. As the final step, a kinematic fit with the D^+ mass as constraint is applied.

The beam-constrained mass distribution[1] of signal candidates from the full sample are shown in fig.1. The distribution is fitted with a phsp motivated shape for the background and a signal shape taken from simulation and convoluted with a Gaussian. In the signal region(light shaded region) 142446±378 signal events are obtained with a purity of 84.9±0.1%. The Dalitz plot is shown in fig.4(a)

3. Partial wave analysis

The matrix element of the decay $K^0_S\pi^+\pi^0$ is described in the isobar model as the sum over all partial waves contributing:

$$\mathscr{M} = \sum_{L=0}^{L_{max}} Z_L F_D^L A_L \tag{3.1}$$

where Z_L is the angular distribution, F_D^L the barrier factor for the decay of the D meson and A_L the partial-wave with angular momentum L:

$$A_L = \sum_R c_R W_R Z_R^L \tag{3.2}$$

Each summand consists of a complex coefficient c_R, the shape of the resonance W_R and the barrier factor for the resonance decay Z_R^L. We consider angular momenta up to L_{max}=3. The resonance shapes are described by Breit-Wigner functions with mass depended width. For the L=0 wave a constant contribution for a non-resonant decay is included which is described by a complex number c_{NR}. A decay through the channel $\bar{\kappa}^0\pi^+$ is parametrized by a complex pole model:

$$W_{\bar{\kappa}^0} = \frac{1}{(\mathscr{R} + i\mathscr{I})^2 - m^2_{K^0_S\pi^0}} \tag{3.3}$$

The complex pole position is given by $\mathscr{R}$ and $\mathscr{I}$.

The efficiency correction is performed using a simulated signal sample which passed the detector simulation, reconstruction procedure and our selection. A track-matching algorithm is applied to sort our mis-reconstructed signal events. The efficiency as function of the position in the Dalitz plot is parameterized by a polynomial and threshold factors.

3.1 Background description

The background contribution to the Dalitz plot is either flat combinatorial background or peaking background from self-cross-feed events. For the latter we use a histogram obtained from simulation. For the combinatorial background, we use the side-bands as indicated in Fig.1 and describe

[1] The D^+ mass calculated from the measured momenta of its daughters and the beam energy.

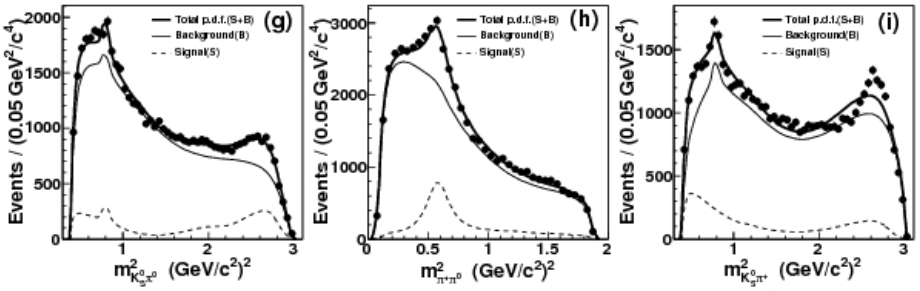

Figure 2: Result of the fit to the full side-band sample.

it by a polynomial. The high side-band includes a significant contribution from signal. This is taken into account by adding an initial signal model to the side-band fit. We then fit the Dalitz plot to obtain an improved signal model and use this model in turn in the side-band fit. This procedure is iterated a couple of times, until the background parameters don't change anymore.

The full side-band sample and our description are shown in fig.2. The deviations at large $m_{K^0_S\pi^+}$ are considered as a systematic error.

3.2 Fit to data

We start fitting the Dalitz plot with all possible intermediate Cabbibo favored resonances. No evidence for doubly Cabbibo suppressed channels is found. Furthermore the contributions from $\bar{K}^*(1410)^0\pi^+$, $\bar{K}^*_2(1430)^0\pi^+$ and $\bar{K}^*_3(1780)^0\pi^+$ are not significant and are not considered in the final model. We test models without NR and/or $\bar{\kappa}\pi^+$ contribution, which reduces the fit quality. Contributions from NR and $\bar{\kappa}\pi^+$ to the $K^0_S\pi^0$ S-wave are found to be present in our data.

The difference of the efficiency correction between MC and data is reduced by a momentum depended correction obtained from control samples. Fig.3 shows the correction for K^0_S and π^0.

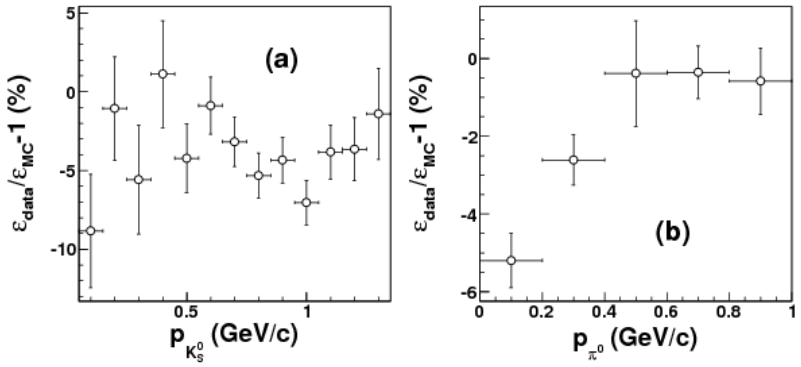

Figure 3: Momentum depended efficiency correction for K^0_S and π^0.

Parameters adjusted in the fit are magnitude and phases of the individual resonances as well as the pole position of the $\bar{\kappa}$ and the mass and width of the $\bar{K}*(1430)$.

The final model is listed in Tab.1 and the Dalitz plot together with our amplitude model is shown in fig.4.

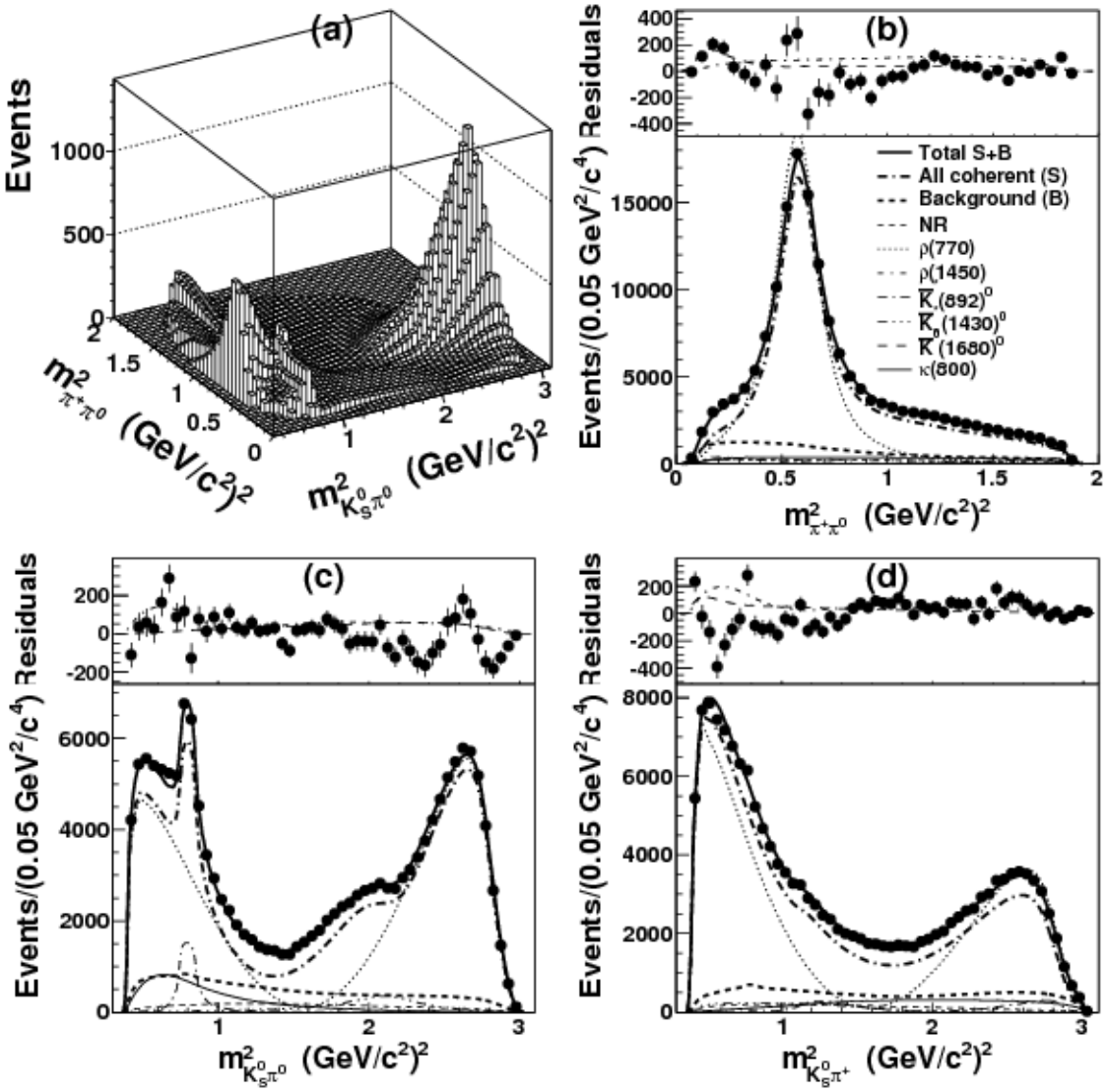

Figure 4: The results of fitting

3.3 (Quasi-)Model independent PWA

Model dependence of Dalitz plot analyses is always an issue. The NR and $\bar{\kappa}\pi^+$ contribution to the $K^0_S\pi^0$ S-wave are not well established and therefore we cross-check our result using a (quasi-) model-independent analysis of the S-wave. We substitute the contributions of interest in the first partial-wave by a mass depended complex number:

$$W(m_{K^0_S\pi^0}) = a(m_{K^0_S\pi^0})e^{i\phi(m_{K^0_S\pi^0})} \qquad (3.4)$$

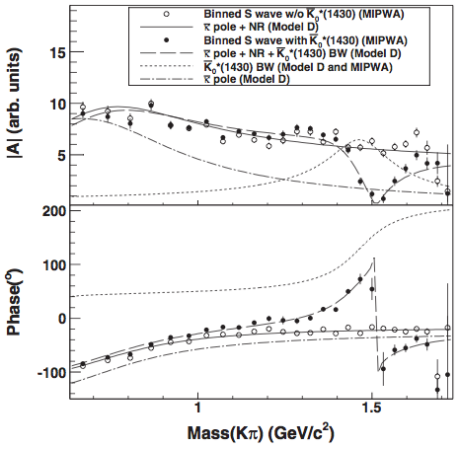

Figure 5: Result of (quasi-) model-independent analysis.

We calculate the values for $a(m_{K^0_S\pi^0})$ and $\phi(m_{K^0_S\pi^0})$ in $m_{K^0_S\pi^0}$ mass bins (full dots) and compare it to our final model (long dashed line) in Fig.5. Both approaches agree well.

4. Systematic uncertainties

We expect contributions to the systematic uncertainty from the background description, from the efficiency correction and from the model dependence of our amplitude. The separated uncertainties as well as the total uncertainty are shown in Tab.1.

4.1 Background

We studied uncertainties from the shape of the background and from the absolute normalization. The background shape is studied by using an alternate background description using a histogram p.d.f. from the low mass side-band sample. We compare the fit result obtained with the histogram p.d.f. with the result obtained using the parametrized background shape. The difference is taken as systematic error. The final fit uses high and low mass side-bands. We add the deviations to the systematic uncertainty that occurs when using high or low sideband data only. Systematics on the background yield are determined by changing the signal ratio by one standard deviation.

4.2 Efficiency

The uncertainty in the efficiency correction comes from the parameterization as well as from the difference between data and MC. The influence of the parametrization is determined by using a smoothed efficiency histogram instead of the parametrization as alternate efficiency correction in the fit. Furthermore we obtain the efficiency from a flat PHSP sample instead of from a sample with resonant substructure. The uncertainty due to the momentum-depended efficiency correction is assumed to be not larger then the rms of the correction values. A difference between data and MC which is not momentum depended does not influence our result. Also the influence of the finite resolution of the Dalitz variables is included.

4.3 Model

The model dependence is studied by changing the parametrization of the resonances (e.g. different type of barrier factor). This contribution is listed as 'Shape' in Tab.1. The choice of the final set of resonance is another source of systematic uncertainty and is listed as 'Add'. The uncertainty is evaluated by comparing different sets.

5. Summary

We analyze the decay $D^+ \to K^0_S\pi^0\pi^+$ with the full BESIII dataset of $2.92\,\mathrm{fb}^{-1}$ at $\sqrt{s} = 3.77\,\mathrm{GeV}$. We select 166694 signal candidates with a background level of 15.1%.

We found that the Dalitz plot is well described by an isobar model with 6 intermediate resonances [$K^0_S\rho^+$, $K^0_S\phi(1450)$, $\bar{K}^{*0}$, $\bar{K}_0(1430)^0$, $\bar{K}(1680^0\pi^+$, $\bar{\kappa}^0\pi^+$]. The channel $\bar{\kappa}\pi^+$ significantly contributes to the $K^0_S\pi^0$ S-wave. We measure its complex pole position to be $(752 \pm 15 \pm 69^{+55}_{-73}, -229 \pm 21 \pm 44^{+40}_{-55})$MeV. Furthermore we find contributions from non-resonant decay and from $\bar{K}^*(1430)\pi^+$. The $K^0_S\pi^0$ S-wave takes account for 17.3% of the intensity. The results agree

Parameters	Value	Statistical errors	Experimental errors			Modeling errors		
			Background	Efficiency	Total	Shape	Add	Total
NR FF (%)	4.6	0.7	3.5	1.0	3.6	$^{+2.9}_{-1.5}$	$^{+2.7}_{-3.3}$	$^{+4.0}_{-3.6}$
NR phase (°)	279	6	5	15	15	$^{+6}_{-25}$	$^{+22}_{-12}$	$^{+23}_{-27}$
$\rho(770)^+$ FF (%)	83.4	2.2	2.7	0.7	2.8	$^{+1.1}_{-1.9}$	$^{+6.4}_{-1.1}$	$^{+6.5}_{-2.2}$
$\rho(1450)^+$ FF (%)	2.1	0.3	0.9	0.9	1.2	$^{+0.7}_{-0.1}$	$^{+0.8}_{-1.5}$	$^{+1.0}_{-1.5}$
$\rho(1450)^+$ phase (°)	187	3	4	4	5	$^{+9}_{-15}$	$^{+26}_{-5}$	$^{+28}_{-16}$
$\bar{K}^*(892)^0$ FF (%)	3.58	0.17	0.12	0.11	0.17	$^{+0.31}_{-0.18}$	$^{+0.16}_{-0.28}$	$^{+0.35}_{-0.34}$
$\bar{K}^*(892)^0$ phase (°)	293	2	1	2	2	$^{+2}_{-7}$	$^{+6}_{-2}$	$^{+6}_{-7}$
$\bar{K}^*_0(1430)^0$ FF (%)	3.7	0.6	0.6	0.5	0.8	$^{+0.4}_{-0.3}$	$^{+0.7}_{-0.8}$	0.8
$\bar{K}^*_0(1430)^0$ phase (°)	334	5	8	4	9	$^{+1}_{-10}$	$^{+3}_{-28}$	$^{+3}_{-30}$
$\bar{K}^*(1680)^0$ FF (%)	1.3	0.2	0.6	0.2	0.7	$^{+0.6}_{-0.1}$	$^{+0.1}_{-1.1}$	$^{+0.6}_{-1.1}$
$\bar{K}^*(1680)^0$ phase (°)	252	2	9	6	11	$^{+6}_{-2}$	$^{+7}_{-28}$	$^{+9}_{-28}$
$\bar{\kappa}^0$ FF (%)	7.7	1.2	2.5	3.1	4.0	$^{+2.0}_{-2.7}$	$^{+4.7}_{-0.1}$	$^{+5.1}_{-2.7}$
$\bar{\kappa}^0$ phase (°)	93	7	25	14	28	$^{+14}_{-7}$	$^{+16}_{-22}$	$^{+21}_{-23}$
$NR + \bar{\kappa}^0$ FF (%)	18.6	1.7	1.1	1.0	1.5	$^{+1.6}_{-3.7}$	$^{+0.5}_{-2.3}$	$^{+1.7}_{-4.4}$
$K^0_S\pi^0$ S-wave FF (%)	17.3	1.4	2.1	0.5	2.1	$^{+0.7}_{-3.8}$	$^{+2.6}_{-0.6}$	$^{+2.7}_{-3.8}$

Table 1: Fit result of the final model with systematic uncertainties.

Mode	Partial branching fraction (%)
$D^+ \to K^0_S\pi^+\pi^0$ nonresonant	$0.32 \pm 0.05 \pm 0.25^{+0.28}_{-0.25}$
$D^+ \to \rho^+ K^0_S$, $\rho^+ \to \pi^+\pi^0$	$5.83 \pm 0.16 \pm 0.30^{+0.45}_{-0.15}$
$D^+ \to \rho(1450)^+ K^0_S$, $\rho(1450)^+ \to \pi^+\pi^0$	$0.15 \pm 0.02 \pm 0.09^{+0.07}_{-0.11}$
$D^+ \to \bar{K}^*(892)^0\pi^+$, $\bar{K}^*(892)^0 \to K^0_S\pi^0$	$0.250 \pm 0.012 \pm 0.015^{+0.025}_{-0.024}$
$D^+ \to \bar{K}^*_0(1430)^0\pi^+$, $\bar{K}^*_0(1430)^0 \to K^0_S\pi^0$	$0.26 \pm 0.04 \pm 0.05 \pm 0.06$
$D^+ \to \bar{K}^*(1680)^0\pi^+$, $\bar{K}^*(1680)^0 \to K^0_S\pi^0$	$0.09 \pm 0.01 \pm 0.05^{+0.04}_{-0.08}$
$D^+ \to \bar{\kappa}^0\pi^+$, $\bar{\kappa}^0 \to K^0_S\pi^0$	$0.54 \pm 0.09 \pm 0.28^{+0.36}_{-0.19}$
$NR + \bar{\kappa}^0\pi^+$	$1.30 \pm 0.12 \pm 0.12^{+0.12}_{-0.30}$
$K^0_S\pi^0$ S-wave	$1.21 \pm 0.10 \pm 0.16^{+0.19}_{-0.27}$

Table 2: Partial branching-fractions based on our fit result and the branching ratio $D^+ \to K^0_S\pi^0\pi^+$ from PDG.

with a complementary analysis of CLEO-c in the channel $D^+ \to K^-\pi^+\pi^+$. To minimize model dependence a model independent analysis on the $K^0_S\pi^0$ S-wave is performed. Both approaches agree well. The fit fractions from Tab.1 multiplied with the branching fraction $D^+ \to K^0_S\pi^0\pi^+$ yield the partial branching fractions, as listed in tab.2

References

[1] J. Adler et al. "Resonant substructure in $K\pi\pi$ decays of charmed D mesons". In: *Physics Letters B* 196.1 (Sept. 1987), pp. 107–112.

[2] M. Ablikim et al. "Design and construction of the BESIII detector". In: *Nucl.Instrum.Meth.A* 614.3 (Mar. 2010), pp. 345–399.